14th International Symposium on the Packaging and Transportation of Radioactive Materials (PATRAM 2004), Berlin, Germany, September 20-24, 2004

Paper # 092

Analyses to Demonstrate the Structural Performance of the CASTORÒ KN12 in Hypothetical Accident Drop Accident Scenarios

Rudolf Diersch, Manfred Weiss, Gesellschaft für Nuklear-Behälter mbH, Germany

Chi-Fung Tso, Arup, UK

Sung-Hwan Chung, Heung-Young Lee, KHNP-NETEC, South Korea

INTRODUCTION

CASTOR® KN-12 is a new cask design by GNB for KHNP-NETEC for dry and wet transportation of up to twelve spent PWR fuel assemblies in Korea. It received its transport license from the Korean Competent Authority KINS in July 2002 and is now in use in South Korea.

It has been designed to satisfy the regulatory requirements of the 10 CFR 71 [1] and the IAEA ST-1 [2] for Type B(U)F packages.

Its structural performance was demonstrated against the load cases and boundary conditions as defined in 10 CFR 71 and NRC's Regulatory Guide 7.8 [3], and further explained in NUREG 1617 [4]. This included normal conditions of transport load cases - including Hot Environment, Cold Environment, Increased External Pressure (140MPa), Minimum External Pressure (24.5kPa), Vibration and shock, and 0.3m free drop – and the hypothetical accident conditions load cases – including the 9m Free Drop, Puncture, Thermal Fire Accident, 200m Water Immersion and 1.5x MNOP Internal Pressure.

Structural performance were demonstrated by analysis, including state-of-the-art finite element (FE) simulation, and confirmed by tests using a 1/3-scale model. Test results were also used to verify the numerical tool and the methods used in the analyses. All the structural analyses including validation against drop tests were carried out by Arup, and testing were carried out by KAERI.

This paper concentrates on the analysis carried out to demonstrate performance in the hypothetical accident 9m free drop scenarios, and results from a small selection of them.

DESCRIPTION OF THE CASK

The containment vessel consists of a cylindrical thick-walled forged carbon steel body, closed by a stainless steel lid with thirty-seven M48 studs with nuts and three M48 cap screws and sealed by an elastomer O-ring. The cask cavity and the O-ring seating surfaces are covered by a welded stainless steel cladding for corrosion protection.

In the lid, a vent and drain opening are integrated and closed by a closure plug with an elastomer O-ring seal and covered by the bolted closure lid also sealed with an elastomer O-ring.

Neutron shielding is provided by a polyethylene plate at the bottom side of the cask and two rows of thirty six polyethylene rods residing in longitudinal bore-holes in the cask wall.

Fuel assemblies are located within a fuel basket which consists of rectangular stainless steel receptacles, in a grid work of borated aluminium sheets and spacer units. The borated aluminium plates provide efficient heat removal, and the boron content of these plates assures nuclear criticality safety under normal transportation and under hypothetical accident conditions.

Two pairs of trunnions are attached for lifting, handling and also tie-down during transportation.

Energy absorption and control of deceleration during hypothetical accident 9m drop scenarios are provided by a pair of impact limiters, one at each end of the cask, attached to the cask by bolts during transportation. They are manufactured from a carbon steel plate inner structure and a stainless steel outer shell filled with wood. The outer steel shell is welded water tight to protect the wood against humidity. The steel structure was designed to fully utilise the energy absorbing capacity of the wood.

ANALYSIS METHODOLOGY

There are a number of alternatives methods for the analyses of the hypothetical accident 9m free drop scenario, ranging from "dynamic lumped parameter" method, to quasi-static methods in which the containment and the basket are analysed on their own using static implicit FE analysis, to detailed "all-in" dynamic analysis using non-linear explicit FE methods.

The performance of the CASTOR KN12 in the hypothetical accident drop scenarios was demonstrated by explicit non-linear FE simulation, using a three-dimensional detailed model of the complete package, with the FE code LS-DYNA [5]. This was the best and the most advantageous approach taking into consideration: behaviour of the cask in the drop scenarios, purpose and context of the analyses, requirements of the licensing authority, requirements of the design code, budget and time scale, capability of the analyst and capacity of FE analysis software and hardware.

This is the most robust method, capable of the most realistic and accurate simulation of the behaviour, as it takes into account at the same time: the explicit and realistic representation of the behaviour of the structure and its components, the dynamic nature of the event, the non-linear nature of the deformation of certain cask components and the three dimensional, transient and often non-linear interaction between the components

DROP SCENARIOS

10 CFR 71 requires the structural adequacy be demonstrated for a free drop through a height of 9m onto a flat, unyielding, horizontal surface, striking the surface in a position for which maximum damage is expected.

The cask was evaluated for the following centre of gravity (CG) over initial point of impact orientations:

- Corner - lid edge and base edge drops
- Axis vertical – lid down and base down drops
- Axis horizontal – side drop

as well as oblique drops.

These drop orientations bound the behaviour of the cask in the 9m free drop scenario.

MODELLING

One basic detailed FE model, in combination with different initial and boundary conditions, was used for the analysis of all the CG over point of impact drops and the oblique drop at the worst oblique angle.

The detailed model consists of 360,000 elements and the top half of the model is shown in Figure 1.

The mesh was designed to be appropriate for the purpose of the analysis and for the expected behaviour of the package. It was refined at areas of higher stress gradients, areas of larger deformation gradients, and where a higher level of accuracy was required. It was coarsened elsewhere to keep the overall number of elements to a minimum, as the number of elements directly affects the analysis time.

The lid-body bolts were modelled using solids. The threaded interfaces between the bolt and the cap nut, between the bolt and the bushing, and between the bushing and the body were modelled with continuous meshes across the interfaces.

The mesh of the bolts was a key factor in determining the mesh in the body and the lid at the lid-body interface. The location of the bore holes was the key factor in determining the mesh in the body.

The basket was modelled in extensive detail so that stresses and deflections can be predicted with sufficient accuracy as input into criticality evaluation. All the components – receptacles, borated aluminium plates, and spacers – were modelled explicitly, with a combination of solids and shell elements. Since the behaviour of the cask cavity on which the basket is supported has a significant influence on the behaviour of the basket, the model was designed to ensure that this interface is accurately modelled.

The steel housing and the wood in the impact limiters were modelled separately. The housing was modelling using a combination of shells and solids. The wood in each compartment of the steel housing was modelled as a single "block" of continuous solids. This made best use of the wood crush data that was available. Crush behaviour was modelled using MAT_HONEYCOMB, based on test data from a programme of tests carried out by GNB in 1990. In that programme, cylindrical specimens of a variety of wood species with different grain orientations and with or without a thin steel casing were tested quasi-statically and dynamically by a guided falling mass with a strain rate typical of real regulatory impacts.

Water was modelled using solid elements, with bulk modulus of water but with no shear stiffness. Instead of modelling the water to occupy all the gaps and spaces in the cask cavity between the many components of the basket and fuel assemblies, the whole volume was modelled as a single continuous block of solids, but with no interaction with the basket or the fuel assemblies. For components submerged in water, this is a conservative assumption, as far as loading on them is concerned.

With this modelling method, the volume of water in the model was larger than in reality, because the presence of the components it submerged were ignored. To compensate for this increased volume, the density of the water should be reduced to achieve the correct mass of water. But since water pressure on the cavity walls is proportional to the density of water, reducing the density would lead to a water pressure smaller than that in reality. Hence, the real density of water (1000kg/m^3) was used, achieving the correct water pressure on the cask walls, and conservatively overloading the cask with a heavier than reality mass of water, and similarly, inertia.

In accordance with ASME Boiler and Pressure Vessel Code [6] Section III Division 3, elastic material properties as given in the code were used in the modelling for all the containment components.

The basket was analysed using the plastic analysis method as allowed by ASME Boiler and Pressure Vessel Code Section 3 App F, to obtain a correct or conservative prediction of displacements. Basket components were modelled using elastic-plastic properties with strain hardening. The input properties were derived from the "minimum" properties of the materials specified in ASME Boiler and Pressure Vessel Code Section 2 Part D and Part A. “Minimum” properties were used in order to obtain conservative estimates of deformation.

The unyielding target was modelled using *RIGIDWALL, which allows no penetration and absorbs no energy in impact.

INITIAL CONDITIONS

Each analysis consisted of two phases. Phase 1 was the “dynamic relaxation” phase during which bolt prestresses due to bolt torque were applied to the lid bolts and the closure lid bolts by “dynamic relaxation” to obtain the correct bolt stresses and stresses in the adjacent components. Phase 2 was the transient phase during which the impact was analysed.

At the start of transient phase, for the CG over point of impact drops, the whole cask model was given an initial velocity of 13.3 m/s perpendicular to the target, corresponding the impact velocity after a drop from 9m.

For the oblique drop, instead of prescribing an initial velocity of 13.3m/s to the model and analysing the model at a range of drop orientations, a staged approach was adopted. Using a simplified model which was identical to the detailed model except that the whole cask and its contents were modelled as undeformable, a range of drop angles from 2.5 degrees to 15 degrees was analysed in order to obtain a drop angle at which the velocity at second impact is highest. From the analysis of the simplified model at the worst drop angle, the velocity profile and cask orientation at second impact were obtained. They were then applied to the detailed model as initial conditions. The detailed model was analysed only for the second impact. Snap shots from an oblique drop is shown in Figure 2 and variation of velocity at the top end of the cask with drop angle is shown in Figure 3.

The advantage of this approach was that a larger range of impact angles could be analysed to determine the worst impact angle, hence determining it with greater accuracy than is possible with either hand calculations or with the detailed model.

BEHAVIOUR IN THE SIDE DROP

The side drop is the drop scenario in which the effect of interaction between the cask and the basket is most significant.

During the drop event, the cask body deflects supported at the ends by the impact limiters. Deformation of the top impact limiter is shown in Figure 4.

Globally, the cask body behaves essentially like a beam supported at the ends - creating a tensile axial stress on the face nearest the target, and compressive stress at the opposite face. More locally, bending of the cask wall that is near the target, due to the specific way the impact limiter is slotted into the body and the location of the chamfer on the body where a thicker section transitions into a thinner section. And local compressive stresses at the interface with the interface with the impact limiters on which it is supported. At the top end, this causes the slight ovaling as expected. These are best illustrated by way of direct stress in the lengthwise direction (Z-direct stress) as in Figure 5, and principal stresses at a section near the top of the moderator bore-holes, in Figure 6.

Interaction between the body and the lid at the interface with the top impact limiter is shown in Figure 7. Bearing of the lid onto the body - having taken up the clearance between them - due deflection ("ovaling") of the body at the interface with the top impact limiter and the tendency of the lid to "slide" with respect to the body, put the lid bolts nearest the target into shear, as shown in Figure 8.

The basket is supported on the inner cavity of the cask body. Deflection of the cask body especially deflection of the surface on which the basket is supported has a significant influence on the behaviour of the basket. Behaviour of the basket (borated aluminium plates not shown for clarity) is shown in terms of Von Mises stress in Figure 9 (note that the lower face which is in contact with the cask cavity is shown as upward facing in the figure). The highest stresses can be found at the top and bottom ends where it is "best" supported by the cask's inner cavity, corresponding to the deflections in the cask body as shown in Figure 5 above – due to the way the impact limiters were slotted into the body and the location of the chamfer on the body where the wall thickness changed. Stresses emanating from these supports are shown in Figure 10. The other areas of higher stresses were caused by the overall bending of the basket, and to location of connectors which have small sections compare with the parts they connect.

Because the diameter of the basket was smaller than the inner diameter of the cask cavity, the basket tended to ovalise onto the cavity which itself also tend to ovalise as it decelerated against the impact limiters. The connectors at the perimeter of the basket section tried to minimise the ovaling of the cross section.

BEHAVIOUR IN THE LID EDGE DROP

Deformation of the impact limiter housing is shown in Figure 11. Compressive stresses in the lid edge are shown in terms of minimum principal stress in Figure 12. The localised stresses seen at the edge of the lid are due to compression from the radial ribs in the limiter. The stresses were due to a combination of local stresses at contact with the impact limiter, contact between the lid and the body as the lid, and compression as the cask decelerates. Supported offered by the limiter at the impact edge causes the lid to pivot about that edge. The loading due to its own inertia and those of the contents caused the lid to deflect outwards (Figure 13), but restrained by the bolts, with highest bolt tensile at the far edge, and smallest at the near edge (Figure 14).

Overall stresses in the basket (excluding Bo Al plates and any bar components) are shown in Figure 15, illustrating the higher stresses at the lid edge corresponding to the deformation of the cask wall and the lid in this drop scenario.

EVALUATION OF PERFORMANCE

Stresses in the containment from all the analysis of all the drop scenarios were evaluated against the stress limits specified in ASME Boiler and Pressure Vessel Code. The stresses were below the limits with sufficient margin in all cases.

Displacements between adjacent fuel assemblies – in the order of a tenth of a mm - were obtained from the analyses and provided for criticality evaluation. Criticality performance was shown to be satisfactory in all the drop scenarios.

VERIFICATION AGAINST DROP TESTS

Drop tests on a 1/3-scale model cask were carried out as a means to verifying the numerical tool and the modelling methodology used in the analyses. In order to provide a robust basis for verification, FE analyses of the 1/3-scale model cask in all the drop test scenarios were carried out. In order that the verification of the FE analyses of the 1/3-scale model cask can be extended to the FE analyses of the full scale cask, the same numerical tool and modelling methodology was employed in both.

Taking all the analyses of the 1/3-scale cask into account, the analyses consistently and conservatively over-predicted test results. The behaviour of the package as simulated by analysis was also consistent with the behaviour shown in the tests. The correlation with drop test results thus demonstrated that the modelling methodology and the numerical tool used in the FE analyses were robust, and were reliable in correctly simulating and predicting the behaviour of the full scale cask.

CONCLUSIONS

The work has demonstrated the benefit of employing detailed three-dimensional modelling by explicit non-linear FE simulation in demonstrating the performance of the CASTOR KN12 and its compliance with regulatory requirements in hypothetical accident drop scenarios.

REFERENCES

[1] Title 10 of the Code of Federal Regulations Part 71 (10 CFR Part 71), Packaging and Transportation of Radioactive Materials, April 1996

[2] International Atomic Energy Agency, Regulations for the Safe Transport of Radioactive Material, Safety Standards Series ST-1, 1996 Edition

[3] U.S. Nuclear Regulatory Commission, Load Combinations for the Structural Analysis of Shipping Casks for Radioactive Material, Regulatory Guide 7.8, Rev 1, March 1989

[4] U.S. Nuclear Regulatory Commission, Standard Review Plan for Transportation Packages for Spent Nuclear Fuel: Final Report, NUREG-1617, March 2000

[5] Livermore Software Technology Corporation, LS-DYNA Keyword User's Manual, Version 950, May 1999

[6] American Society of Mechanical Engineers, Boiler and Pressure Vessel Code, 2001.

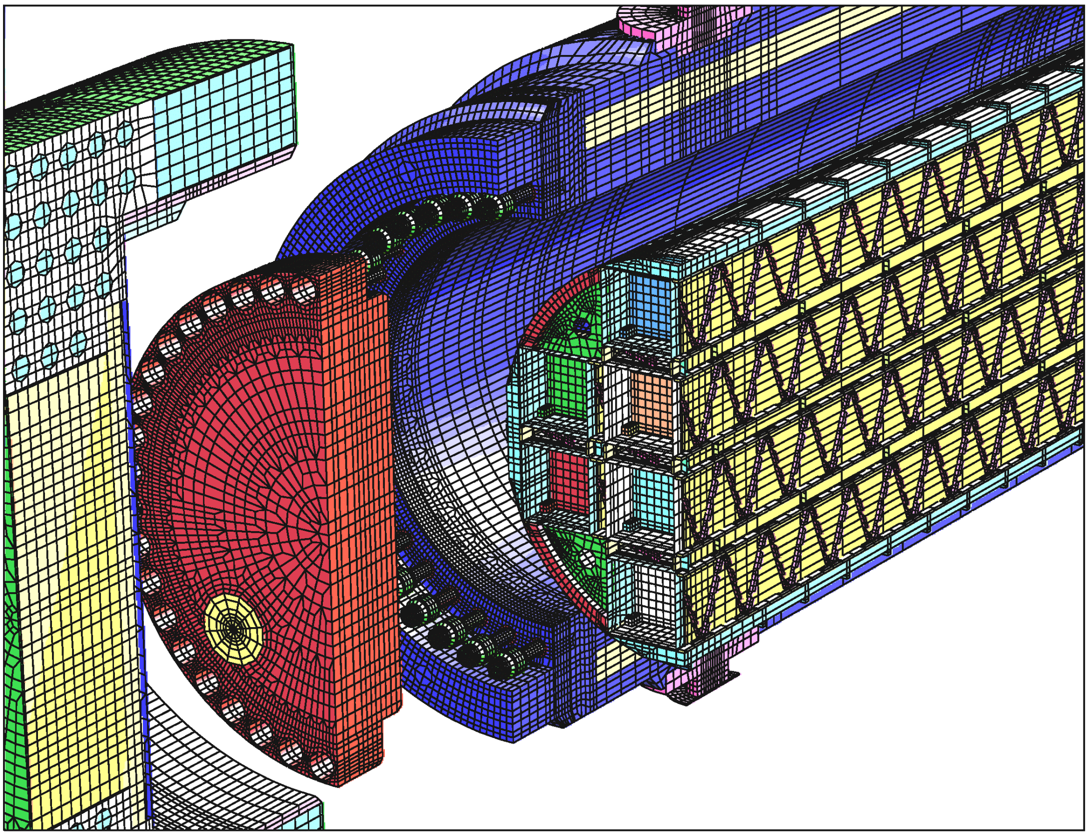

Figure 1 The finite element model

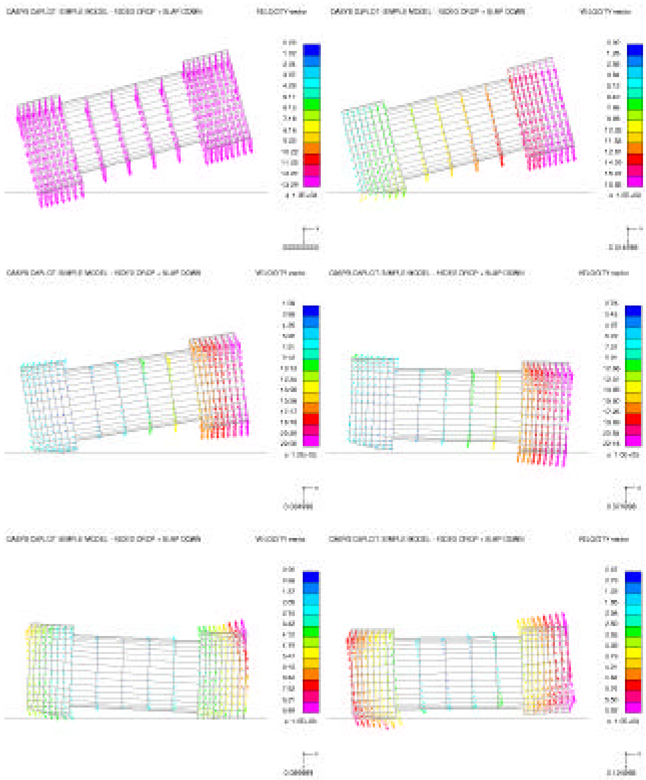

Figure 2 Snap shots of an oblique drop event as analysed using the simplified model

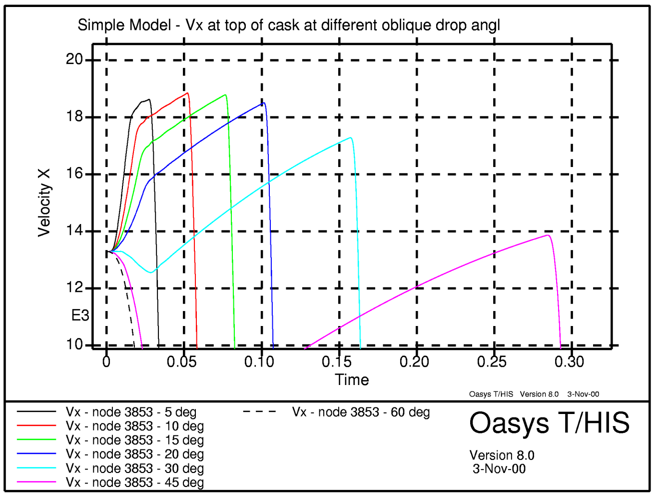

Figure 3 Variation of velocity at the top end of the cask with oblique drop angle

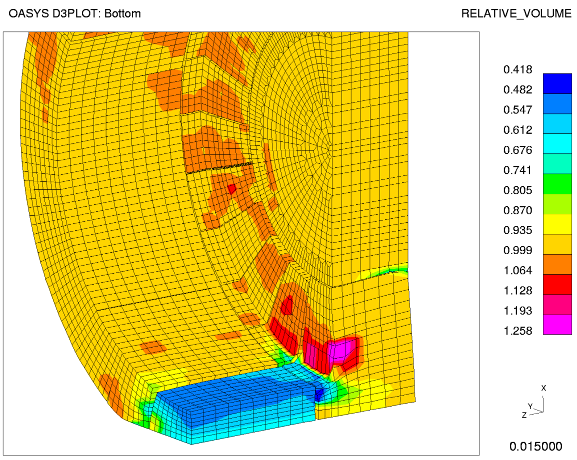

Figure 4 Deformation in the wood of the top impact limiter in the 9m side drop

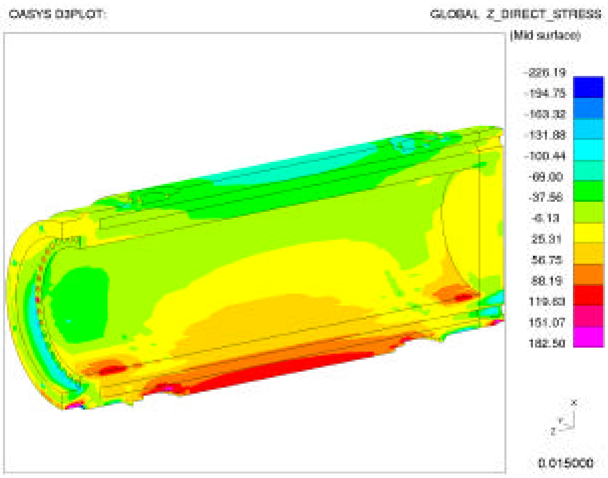

Figure 5 Stresses in the cask body in the 9m side drop

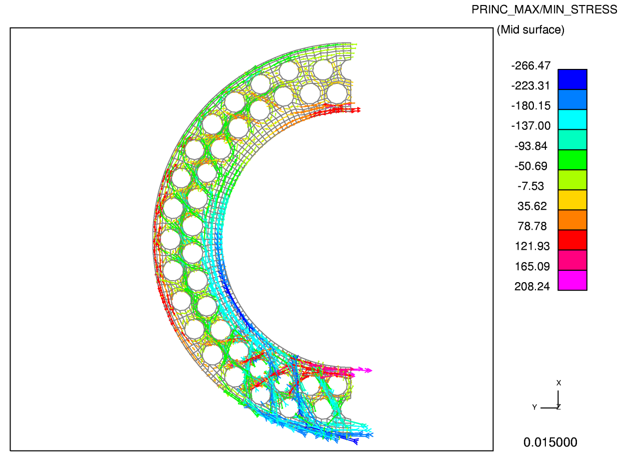

Figure 6 Stresses of a cross section near the top of the bore holes in the 9m side drop

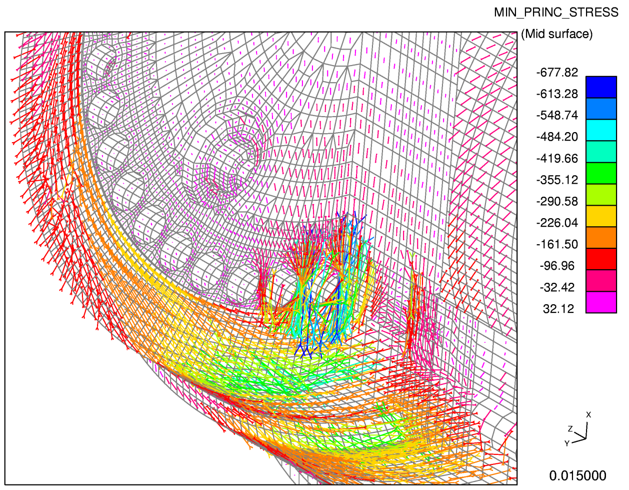

Figure 7 Interaction between the lid and the body in the 9m side drop

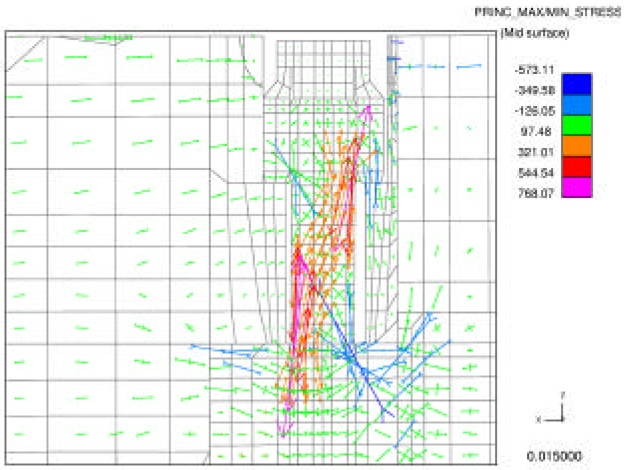

Figure 8 Deflection behaviour of a bolt nearest the target in the 9m side drop

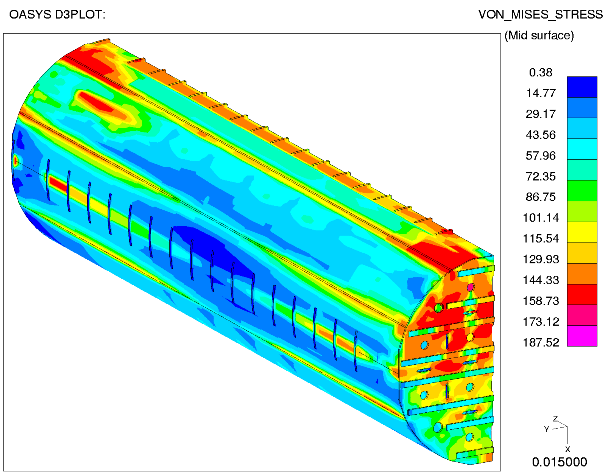

Figure 9 Stresses in the basket in the 9m side drop

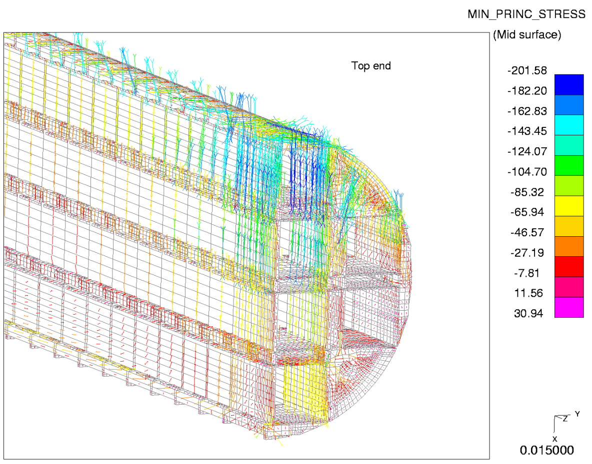

Figure 10 Load path from the support at the cavity into the internals of the basket in the 9m side drop

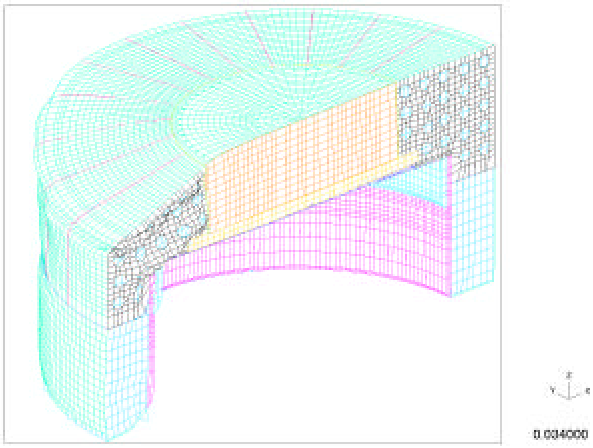

Figure 11 Deformation of the top impact limiter in the 9m lid edge drop

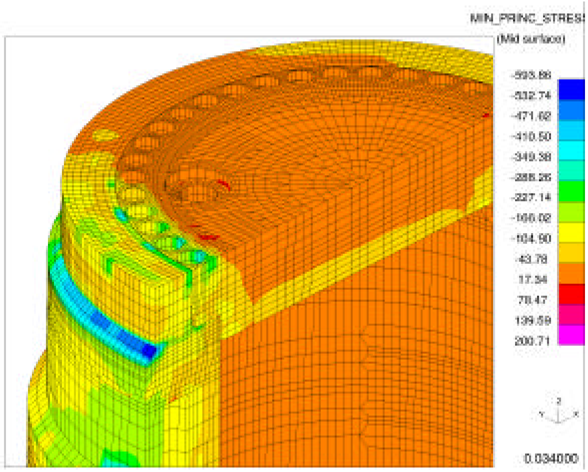

Figure 12 Lid-body interaction and loading from the impact limiter at the contact with the impact limiter in the 9m lid edge drop

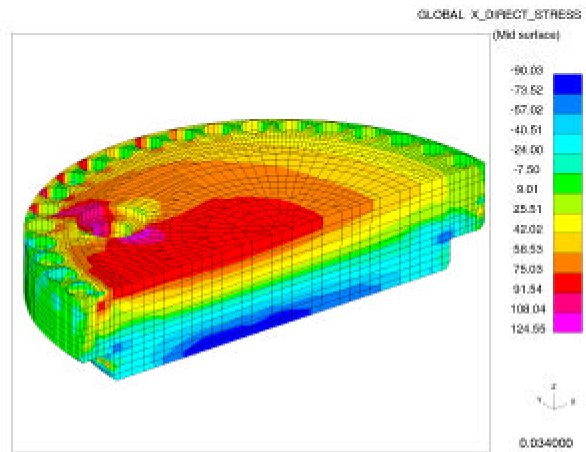

Figure 13 Lid bending deflection behaviour in the 9m lid edge drop

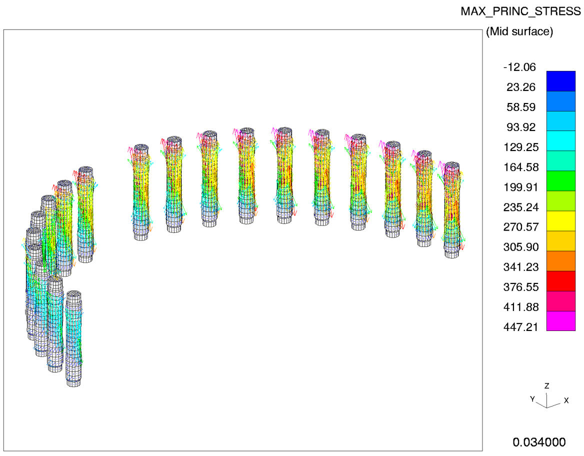

Figure 14 Overall bolt behaviour in the 9m lid edge drop

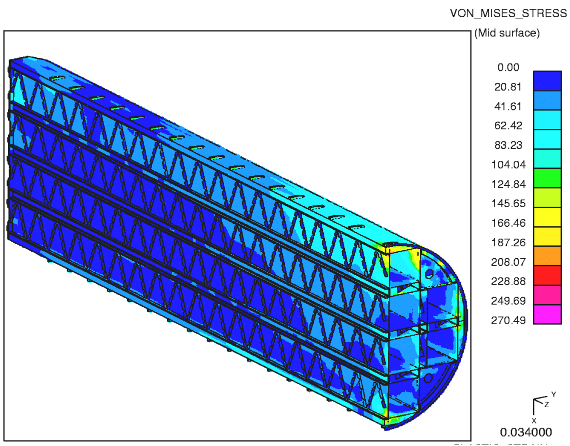

Figure 15 Stresses in the basket in the 9m lid edge drop